

# Optical spin pumping of modulation-doped electrons probed by a two-color Kerr rotation technique

H. Hoffmann,<sup>1</sup> G. V. Astakhov,<sup>1,2,\*</sup> T. Kiessling,<sup>1</sup> W. Ossau,<sup>1</sup> G. Karczewski,<sup>3</sup> T. Wojtowicz,<sup>3</sup> J. Kossut,<sup>3</sup> and L. W. Molenkamp<sup>1</sup>

<sup>1</sup>Physikalisches Institut (EP3), Universität Würzburg, 97074 Würzburg, Germany

<sup>2</sup>A.F. Ioffe Physico-Technical Institute, Russian Academy of Sciences, 194021 St. Petersburg, Russia

<sup>3</sup>Institute of Physics, Polish Academy of Sciences, 02668 Warsaw, Poland

(Received 20 April 2006; revised manuscript received 9 June 2006; published 21 August 2006)

We report on optical spin pumping of modulation electrons in CdTe-based quantum wells with low intrinsic electron density (by  $10^{10} \text{ cm}^{-2}$ ). Under continuous-wave excitation, we reach a steady-state accumulated spin density of about  $10^8 \text{ cm}^{-2}$ . Using a two-color Hanle-MOKE technique, we find a spin-relaxation time of 34 ns in the nearly unperturbed electron gas. Independent variation of the pump and probe energies demonstrates the presence of additional electrons in the quantum well, whose spin-relaxation time is substantially shorter.

DOI: [10.1103/PhysRevB.74.073407](https://doi.org/10.1103/PhysRevB.74.073407)

PACS number(s): 72.25.Fe, 78.66.Hf, 76.30.Pk

The idea to use the spin of electrons and nuclei rather than the electron charge for information processing<sup>1</sup> has renewed the interest in spin-related phenomena in solids. Spin-based concepts for semiconductor devices require the preparation of a long-lived spin state. Diluted magnetic semiconductors (DMS) exhibit a giant Zeeman splitting, enabling efficient spin selection and injection.<sup>2-4</sup> An advantage of the II-VI semiconductors is that the magnetic impurities, such as Mn or Cr, are incorporated *isoelectronically*. This enables the fabrication of high-quality DMS structures whose magnetic and electronic properties can be varied independently. II-VI semiconductors such as ZnSe or CdTe, whose growth procedure is well optimized, are thus well suited for spin-coherence studies. Most current work in this direction, however, concentrates on GaAs. For example, a spin memory of free electrons in excess of 100 ns has been reported for bulk *n*-GaAs.<sup>5,6</sup> For II-VI's, the longest-lived spin polarization reported so far is by two orders of magnitude shorter and was observed in heavily doped<sup>7</sup> and later in undoped<sup>8</sup> ZnSe quantum wells (QWs).

In strongly conducting samples, the D'yakonov-Perel' (DP) mechanism<sup>9</sup> dominates the spin relaxation. This mechanism is quenched for weakly doped, insulating samples when the electrons are localized. In this case, the hyperfine interaction with the nuclei may result in an extended spin coherence,<sup>10</sup> which can be controlled by electron-electron interactions. Calculations show a nonmonotonic behavior for the spin-relaxation time versus doping concentration and suggest that a maximum occurs in the intermediate doping regime, at the onset of the insulator phase.<sup>11</sup> QWs are attractive for such studies, as modulation doping provides a wide-range variation of the intrinsic electron concentration  $n_e$ . The properties of the quasi-two-dimensional electron gas (2DEG) can be monitored through the optical density of neutral excitons ( $X$ ) and negatively charged trions ( $T$ ).<sup>12-14</sup> For slightly doped CdTe QWs, spin-relaxation times of 19 ns (Ref. 15) and 30 ns (Ref. 16) in CdTe QWs have recently been reported, exceeding those for comparable GaAs QWs.<sup>17</sup>

In the present paper we report on further experiments on efficient spin pumping of intrinsically present modulation-doped electrons in CdTe-based QWs. The samples used for our studies are insulating, with a 2DEG density on the order

of  $10^{10} \text{ cm}^{-2}$ . We use a highly sensitive technique, basically a two-color magneto-optical Kerr effect (MOKE) experiment in combination with a Hanle experiment, to probe the net-spin polarization under continuous wave (cw) excitation.<sup>18,19</sup> The Hanle effect (the decrease of polarization under the application of in-plane magnetic fields) gives a characteristic magnetic field  $B_{1/2}$  for the depolarization of the 2DEG, which directly yields the spin-relaxation time  $\tau_s$ .<sup>9</sup> We find that the two-color Hanle-MOKE experiment is a very sensitive tool for measuring spin relaxation and produces an easily observable signal even at very weak illumination. The technique avoids pulsed excitation and, thus, allows a determination of  $\tau_s$  for a nearly unperturbed 2DEG.

For cw pumping, a tunable dye laser is used. The excitation is modulated between  $\sigma^+$  and  $\sigma^-$  circular polarizations at a frequency of 50 kHz using a photoelastic quartz modulator. The degree of circular polarization of the photoluminescence (PL) is detected by a Si-based avalanche photodiode and a two-channel photon counter. The net-spin polarization is probed using a linearly polarized cw Ti:sapphire laser. The photoinduced Kerr rotation  $\theta$  is measured by a balanced diode detector and demodulated by a lock-in amplifier. Both pump and probe beams are focused to the same  $d \approx 300$   $\mu\text{m}$ -diam spot. An external magnetic field can be applied in the sample plane (Voigt geometry). All experiments are carried out at a temperature of 1.8 K; the samples are immersed in superfluid helium.

The samples have been grown by molecular-beam epitaxy on a (100)-oriented GaAs substrate. We present data for five 200-Å-wide CdTe/Cd<sub>0.78</sub>Mg<sub>0.22</sub>Te multiple quantum wells (MQWs) [see the inset in Fig. 1(a)]. The samples are nominally undoped. The low-density 2DEGs in the CdTe MQWs are due to residual *n*-type doping of the Cd<sub>0.78</sub>Mg<sub>0.22</sub>Te barrier. Characteristic PL and reflectivity spectra in the excitonic region of the MQWs are shown in Fig. 1(a). A pair of resonances associated with the neutral exciton ( $X$ ) and negatively charged trion ( $T$ ) is well resolved.<sup>12,20</sup> From the trion-to-exciton ratio of the oscillator strength in the reflectivity spectrum, we estimate the concentration of modulation-doped electrons at  $n_e = 1.3 \times 10^{10} \text{ cm}^{-2}$  (Ref. 21). The narrow inhomogeneous broadening of 0.6 meV of the  $X$  and  $T$  lines is indicative of the high quality of the sample.

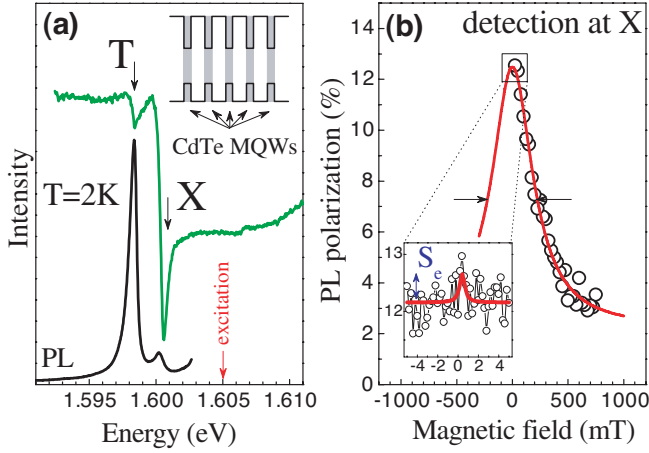


FIG. 1. (Color online) (a) Photoluminescence and reflectivity spectra of 200-Å-wide CdTe/Cd<sub>0.78</sub>Mg<sub>0.22</sub>Te MQWs. PL is recorded under quasiresonant excitation with energy  $E_{pump} = 1.605$  eV. The trion ( $T$ ) and exciton ( $X$ ) resonances are labeled by arrows. Inset: scheme of the structure. (b) Hanle polarization data detected at the exciton luminescence line. The solid line is a Lorentzian fit with  $B'_{1/2} = 220$  mT. Inset: enlarged scale for low fields. The values are  $T = 2$  K,  $P_{pump} = 20$  mW, and  $n_e = 1.3 \times 10^{10}$  cm<sup>-2</sup>.

The key results of the optical spin-pumping experiments are collected in Fig. 2. Panel (a) shows the Hanle-MOKE signal for a pump energy slightly above, and a probe energy slightly below, the trion transition. The Kerr rotation angle  $\theta$  (and thus the spin polarization) completely vanishes with the magnetic field following a Lorentzian

$$\theta = \frac{\theta_i}{1 + (B/B_{1/2})^2}, \quad (1)$$

with  $B_{1/2} = 0.23$  mT. Here,  $\theta_i$  is proportional to the number of pumped spins in the zero magnetic field  $B = 0$  and increases with rising excitation power [Fig. 2(b)].

Equation (1) allows us to determine  $\tau_s$  from the experiment. The application of an external magnetic field  $B$  in the sample plane results in spin precession of the electron spin around the applied field with Larmor frequency  $\omega_L = |g_e| \mu_B B / \hbar$ . Here,  $g_e$  is the electron  $g$  factor. The time evolution of the spin polarization upon delta-pulse excitation can be expressed as  $\theta(t) = \theta_i \cos(\omega_L t) \exp(-t/T_s)$ , where the spin lifetime  $T_s$  is related to, but not necessarily equal to, the intrinsic spin-memory time  $\tau_s$ . For the cw limit one needs to integrate over time, which immediately leads to Eq. (1) with  $B/B_{1/2} = \omega_L T_s$ .<sup>9</sup> Thus, one directly obtains  $T_s = \hbar / (|g_e| \mu_B B_{1/2})$ . With  $g_e = -1.64$ ,<sup>22</sup> the characteristic magnetic field  $B_{1/2} = 0.23$  mT corresponds to  $T_s = 30$  ns [Fig. 2(a)]. The exact relationship between the  $T_s$  and the spin-relaxation time  $\tau_s$  of the unperturbed 2DEG depends on the pump power  $P_{pump}$  and is discussed below. However, it is obvious that  $T_s \rightarrow \tau_s$  as  $P_{pump} \rightarrow 0$ . The data in Fig. 2(c) suggest that  $T_s$  obtained with  $P_{pump} = 0.1$  mW corresponds to the low-power limit with  $\tau_s \geq 30$  ns.

Let us now describe the details of the spin pumping process. Because of the optical selection rules, a circularly polarized photon creates a spin-polarized electron.<sup>9</sup> When these

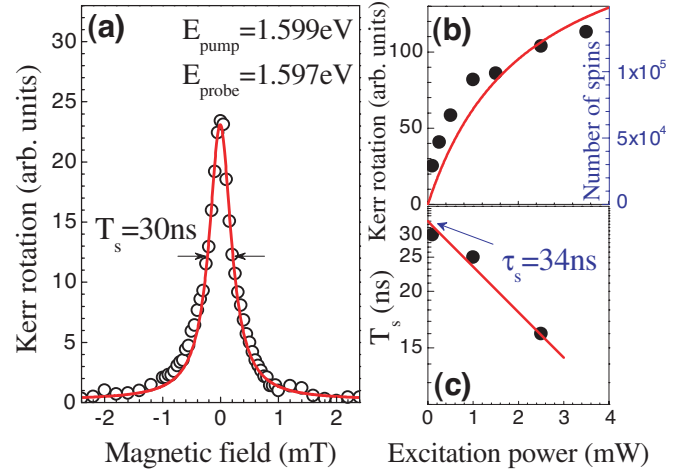


FIG. 2. (Color online) (a) The Hanle-MOKE signal, excited above ( $E_{pump} = 1.599$  eV), and detected below, the trion transition ( $E_{probe} = 1.597$  eV) in the low-power limit ( $P_{pump} = 0.1$  mW). The symbols are experimental points; the line is a fit with Eq. (1). (b) The Kerr rotation angle  $\theta_i$  at zero applied field, which is proportional to the number of spins  $N_s$ , as a function of excitation power. The drawn line is a fit using Eq. (4). (c) Spin lifetime  $T_s$  as a function of excitation power. Following Eq. (3), one extrapolates in the limit  $P_{pump} \rightarrow 0$  to  $\tau_s = 34$  ns.

polarized electrons replace the previously present unpolarized electrons in the MQW, an effective spin pumping of the 2DEG occurs. Under resonant excitation, possible mechanisms are, e.g., spin-dependent formation of the trion singlet state, and electron-exchange scattering of the exciton state. A detailed consideration of these mechanisms is beyond the scope of the present work. Lumped together, these processes can be modeled by the introduction of  $S_e$ , the maximum obtainable photoinduced spin polarization of the 2DEG in the saturation regime. Following the approach for  $n$ -GaAs (outlined in Refs. 6 and 9), the spin pumping-rate equations (at zero magnetic field) can be written as

$$\frac{\partial(n_e S)}{\partial t} = G S_e - \frac{n_e S}{\tau_J} - \frac{S}{\tau_s} n_e, \quad \frac{\partial n_e}{\partial t} = G - \frac{n_e}{\tau_J}. \quad (2)$$

The generation rate  $G$  is proportional to the excitation power ( $G = \gamma P_{pump}$ ), where  $\gamma$  is a coefficient that depends on spot size and absorption efficiency.  $S$  is the actual spin polarization of the 2DEG at a given  $G$ . The time  $\tau_J$  characterizes the spin-transfer rate from the 2DEG back to the exciton or trion reservoir. Under steady-state conditions, Eqs. (2) yield  $\tau_J^{-1} = \gamma P_{pump} / n_e$  and  $S = S_e T_s / \tau_J$ , where

$$T_s^{-1} = \tau_s^{-1} + \frac{\gamma P_{pump}}{n_e}. \quad (3)$$

Following Eq. (3), an extrapolation of  $T_s$  to zero  $P_{pump}$  [the solid line in Fig. 2(c)] yields the intrinsic spin-relaxation time of the 2DEG,  $\tau_s = 34$  ns.

The (zero-field) Kerr rotation angle  $\theta_i$  is proportional to  $\theta_i = \alpha S n_e$ , where  $\alpha$  is a function of the detection energy  $E_{probe}$ . Collecting terms, we have

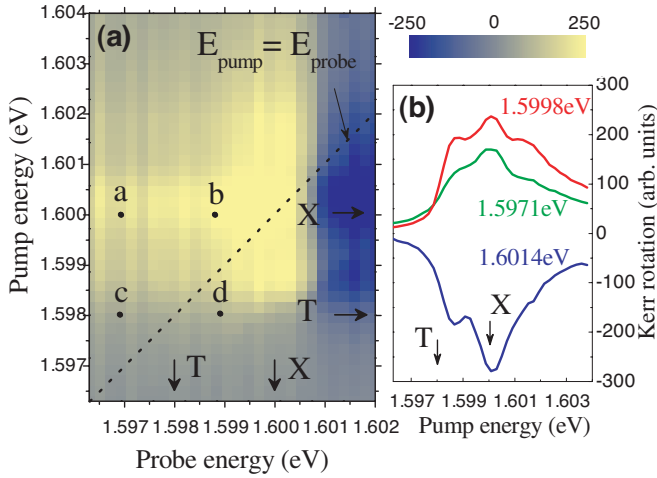


FIG. 3. (Color online) (a) 3D plot of the Kerr rotation angle  $\theta_i$  (at zero magnetic field) as a function of pump ( $E_{pump}$ ) and probe ( $E_{probe}$ ) energies. The trion and exciton transitions are indicated by arrows. Points  $a$ ,  $b$ ,  $c$ , and  $d$  correspond to the similarly labeled panels in Fig. 4. (b) Spectra of the 2DEG spin-polarization excitation (SPE) detected at different energies ( $E_{probe} = 1.5971, 1.5998, 1.6014$  eV).

$$\theta_i = \alpha \frac{\gamma P_{pump} \tau_s}{n_e + \gamma P_{pump} \tau_s} S_e n_e. \quad (4)$$

Equation (4) describes the experimental dependence of  $\theta_i$  on  $P_{pump}$  very well. Fitting the experimental data in Figs. 2(b) and 2(c), we find that  $P_{pump} = 2.2$  mW corresponds to  $\gamma P_{pump} \tau_s = n_e$ . In the arbitrary units of Fig. 2(b),  $\alpha S_e n_e$  corresponds to 200.

For comparison with our two-color technique, we also measured the “classical” Hanle curve, analyzing the polarization of the PL at the X emission line. The PL was excited 5 meV above the exciton transition at  $E_{pump} = 1.605$  eV [Fig. 1(a)]. As the exciton binding energy exceeds 10 meV, excitons rather than unbound electron-hole pairs are created. The Hanle data is shown in Fig. 1(b) and again is well described by Eq. (1) but with  $B'_{1/2} = 220$  mT. Note that in this experiment the electron Hanle signal rides on a constant background, probably due to the field-independent hole polarization. The formal use of  $T'_s = \hbar / (|g_e| \mu_B B'_{1/2})$  with  $g_e = -1.64$  yields  $T'_s = 33$  ps. The difference between  $B_{1/2}$  and  $B'_{1/2}$  by three orders of magnitude is not surprising. An electron-spin precession and relaxation in the exciton may be strongly affected by interaction with a hole, and thus it cannot be directly compared with that of an electron in the 2DEG.

Nevertheless, the photoinduced spin polarization of the 2DEG  $S_e$  also manifests itself in the classical Hanle curve owing to the spin-dependent formation of the trion from the exciton. This contribution is revealed as a narrow peak appearing on the top of the exciton Hanle curve, and has previously been observed in GaAs QWs.<sup>17</sup> However, upon testing many CdTe-based samples,<sup>15</sup> we find that this peak is frequently weak. The signal related to the 2DEG polarization in particular studied samples is enlarged in the inset of Fig. 1(b). This data is difficult to analyze and a value  $S_e \sim 0.5\%$  can only be estimated as an upper limit. We use this value

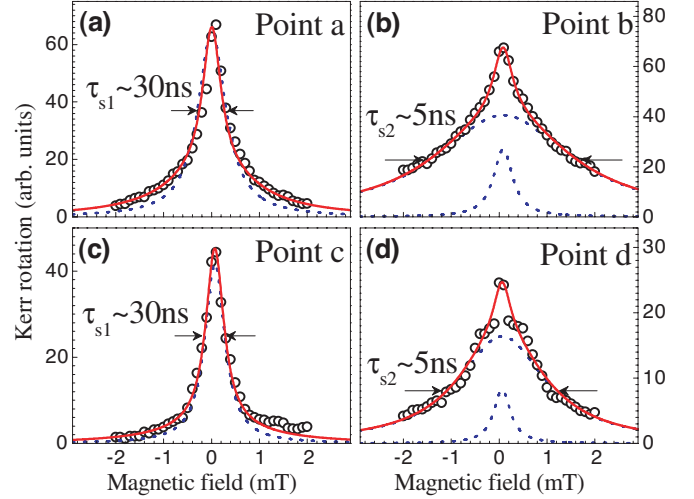


FIG. 4. (Color online) The Hanle-MOKE for different excitation and detection energies [see also the points in Fig. 3(a)]. Symbols are experimental points, solid lines are fits with Eq. (5), and dotted lines are fits with Eq. (1). Fitting parameters are collected in Table I. (a)  $E_{pump} = 1.600$  eV and  $E_{probe} = 1.597$  eV. (b)  $E_{pump} = 1.600$  eV and  $E_{probe} = 1.599$  eV. (c)  $E_{pump} = 1.598$  eV and  $E_{probe} = 1.597$  eV. (d)  $E_{pump} = 1.598$  eV and  $E_{probe} = 1.599$  eV. Excitation and detection power is  $P_{pump} = 0.25$  mW,  $P_{probe} = 0.17$  mW.

(obtained at  $P_{pump} = 20$  mW) for deducing the effective number of probed spins  $N_S$ , which is  $N_S = 5\pi(d/2)^2 S_e n_e$  at high-excitation power ( $P_{pump} \gg 2.2$  mW). Assuming a spot size  $d \sim 300$   $\mu\text{m}$  we obtain  $N_S \sim 2 \times 10^5$ . This value can be related to the saturation level and thus enables the calibration of our Kerr signal to a number of spins [right axis in Fig. 2(b)]. Remarkably, the MOKE significantly improves the sensitivity, allowing us to detect as few as  $10^4$  spins.

A rough estimate of the exciton recombination time  $\tau_0 \sim 100$  ps (Ref. 23) allows us to obtain the average number of excitons  $\Delta n_X$  during our cw experiment, using  $\Delta n_X = G \tau_0$ . At the characteristic pump power [ $P_{pump} = 2.2$  mW, Fig. 2(b)], where  $G \tau_s = n_e$ , one has  $\Delta n_X = n_e \tau_0 / \tau_s$ . The condition  $\Delta n_X \ll n_e$  is obviously fulfilled, which implies that the cw optical pumping induces spin accumulation.

In an additional set of experiments, we measured the photoinduced spin polarization of the 2DEG for different pump and probe energies near the X- and T-transitions [Fig. 3(a)]. As expected intuitively, the excitation spectrum of the spin polarization (SP), i.e.,  $\theta(E_{pump})$ , follows the optical density (reflectivity spectrum). This is shown more clearly in the cross-section trace in Fig. 3(b). At the same time, the Kerr rotation of the probe,  $\theta(E_{probe})$ , has the opposite sign on the high- and low-energy sides. This behavior is typical for the Kerr rotation when the probe energy passes through a resonance.<sup>24</sup>

In order to demonstrate the advantages of using independent  $E_{pump}$  and  $E_{probe}$  energies (two-color mode), we measured the Hanle-MOKE signal at the points labeled as  $a$ ,  $b$ ,  $c$ , and  $d$  in Fig. 3(a). The resulting Hanle-MOKE curves are shown in Fig. 4. We find that, in general, there can be two contributions to these curves and because of that some of them cannot be described using Eq. (1) (see the dotted lines in Fig. 4). A possible explanation may originate from a spa-

tially inhomogeneous distribution of the electrons.<sup>25</sup> The charged trions are more sensitive to localization (for instance, in the electrostatic potential of ionized donors in the barrier) as compared to their neutral counterparts. As a result, when the detection energy is above the  $T$  transition, only weakly localized electrons are probed. For these electrons an alternative mechanism may dominate the spin relaxation, resulting in a shortening of  $\tau_s$ . More extended studies are required to clarify (or refute) this hypothesis, which is beyond the scope of this paper.

In order to fit all experimental data in Fig. 4, we extend Eq. (1) to include two contributions,

$$\theta = \frac{\theta_i^{(1)}}{1 + (B/B_{1/2}^{(1)})^2} + \frac{\theta_i^{(2)}}{1 + (B/B_{1/2}^{(2)})^2}, \quad (5)$$

which allows us to fit all four cases well (see the solid lines in Fig. 4). The fitting parameters are given in Table I. We observe the following tendency in the data: For detection below the trion transition (1.598 eV) at (points  $a$  and  $c$ ,  $E_{probe}=1.597$  eV), the spin-relaxation time is  $\tau_s^{(1)}=30\pm 2$  ns. Shifting the detection energy only 2 meV higher (points  $b$  and  $d$ ,  $E_{probe}=1.599$  eV), but above the trion transition, we observe a dominant contribution with a shorter spin-relaxation time  $\tau_s^{(2)}=5\pm 1$  ns, which we tentatively assign to enhanced DP relaxation of nonlocalized electrons. The relative weight of these contributions (i.e., ratio  $\theta_i^{(2)}/\theta_i^{(1)}$ ) depends only slightly on the pump energy when the probe energy is fixed.

In summary, we report on efficient spin pumping of

TABLE I. Parameters (in brackets) of fits to Eq. (5) [(1)] shown as solid (dotted) lines in Fig. 4. Points  $a$ ,  $b$ ,  $c$ , and  $d$  refer to the  $(E_{pump}, E_{probe})$  pairs indicated in Fig. 3(a).

	Point $a$	Point $b$	Point $c$	Point $d$
$E_{pump} =$	1.600 eV	1.600 eV	1.598 eV	1.598 eV
$E_{probe} =$	1.597 eV	1.599 eV	1.597 eV	1.599 eV
$\theta_i^{(2)}/\theta_i^{(1)}$	0.33 [0]	1.5 [–]	0.08 [0]	1.98 [–]
$B_{1/2}^{(1)}$ (mT)	0.23 [0.35]	0.24	0.23 [0.25]	0.21
$\tau_s^{(1)}$ (ns)	30 [20]	29	30 [28]	32
$B_{1/2}^{(2)}$ (mT)	1.1	1.7	1.3	1.1
$\tau_s^{(2)}$ (ns)	6	4	5	6

modulation-doped electrons in CdTe QWs containing low-density ( $10^{10}$  cm<sup>-2</sup>) insulating 2DEGs. It is monitored using a technique based on the Kerr rotation, which is sensitive to  $10^4$  spins. We obtain a spin-memory time  $\tau_s=34$  ns for an unperturbed 2DEG. We find that our sample exhibits two electron subsystems, whose spin-relaxation time differs by a factor of 6.

The authors thank R. I. Dzhioev, K. V. Kavokin, M. V. Lazarev, and V. L. Korenev, for fruitful discussions. We also acknowledge D. R. Yakovlev and E. A. Zhukov for providing us with their data on time-resolved Kerr rotation before publication.<sup>16</sup> This work was supported by the Deutsche Forschungsgemeinschaft (Grants No. SFB 410 and No. 436 RUS 113/843).

\*Email address: astakhov@physik.uni-wuerzburg.de

<sup>1</sup>G. Prinz, Phys. Today **48**, 58 (1995).

<sup>2</sup>R. Fiederling *et al.*, Nature (London) **402**, 787 (1999).

<sup>3</sup>Y. Ohno *et al.*, Nature (London) **402**, 790 (1999).

<sup>4</sup>A. Slobodskyy *et al.*, Phys. Rev. Lett. **90**, 246601 (2003).

<sup>5</sup>J. M. Kikkawa and D. D. Awschalom, Phys. Rev. Lett. **80**, 4313 (1998).

<sup>6</sup>R. I. Dzhioev *et al.*, Pis'ma Zh. Éksp. Teor. Fiz. **74**, 182 (2001); JETP Lett. **74**, 182 (2001).

<sup>7</sup>J. M. Kikkawa *et al.*, Science **277**, 1284 (1997).

<sup>8</sup>H. Kalt *et al.*, J. Cryst. Growth **214/215**, 630 (2000).

<sup>9</sup>*Optical Orientation*, edited by F. Meyer and B. P. Zakharchenya (North-Holland, Amsterdam, 1984).

<sup>10</sup>R. I. Dzhioev *et al.*, Phys. Rev. Lett. **88**, 256801 (2002).

<sup>11</sup>R. I. Dzhioev *et al.*, Phys. Rev. B **66**, 245204 (2002).

<sup>12</sup>K. Kheng *et al.*, Phys. Rev. Lett. **71**, 1752 (1993).

<sup>13</sup>P. Kossacki *et al.*, Phys. Rev. B **60**, 16018 (1999).

<sup>14</sup>G. V. Astakhov *et al.*, Phys. Rev. B **62**, 10345 (2000).

<sup>15</sup>G. V. Astakhov *et al.*, Phys. Status Solidi B **243**, 858 (2006).

<sup>16</sup>E. A. Zhukov *et al.*, Phys. Status Solidi B **243**, 878 (2006).

<sup>17</sup>R. I. Dzhioev *et al.*, Phys. Rev. B **66**, 153409 (2002).

<sup>18</sup>J. Stephens *et al.*, Phys. Rev. Lett. **93**, 097602 (2004).

<sup>19</sup>S. A. Crooker and D. L. Smith, Phys. Rev. Lett. **94**, 236601 (2005).

<sup>20</sup>G. V. Astakhov *et al.*, Phys. Rev. B **71**, 201312(R) (2005).

<sup>21</sup>G. V. Astakhov *et al.*, Phys. Rev. B **65**, 115310 (2002).

<sup>22</sup>A. A. Sirenko *et al.*, Phys. Rev. B **56**, 2114 (1997).

<sup>23</sup>E. A. Zhukov and D. R. Yakovlev (private communication).

<sup>24</sup>C. Testelin *et al.*, Phys. Rev. B **55**, 2360 (1997).

<sup>25</sup>G. Eytan *et al.*, Phys. Rev. Lett. **81**, 1666 (1998).